ISSN 0015-4628, Fluid Dynamics, 2019, Vol. 54, no. 7, pp. 958–969. © Pleiades Publishing, Ltd., 2019.
Russian Text © The Author(s), 2019, published in Prikladnaya Matematika i Mekhanika, 2019, Vol. 83, No. 3, pp. 452–467.

Numerical Analysis of Flows of Stratified and Homogeneous Fluids near Horizontal and Inclined Plates

Ya. V. Zagumennyi[a],* and Yu. D. Chashechkin[b],**

[a] *Institute of Hydromechanics, National Academy of Sciences of Ukraine, Kiev, 02000 Ukraine*
[b] *Ishlinsky Institute for Problems in Mechanics, Russian Academy of Sciences, Moscow, 119526 Russia*
**e-mail: zagumennyi@gmail.com*
***e-mail: yulidch@gmail.com*

Received March 6, 2019; revised March 19, 2019; accepted April 7, 2019

Abstract—The structure and dynamics of flows near a horizontal and inclined plates in stratified and homogeneous fluids in a transient vortex regime are studied for various angles of inclination of the plate to the horizon and various geometrical modifications of its front and rear edges. This study is based on high-precision numerical modeling of the fundamental system of equations, which allows calculations of both stratified and homogeneous viscous liquids in a unified formulation. Instantaneous patterns of the vorticity fields, pressure gradient, and density, as well as the values of forces and moments acting on the surface of the plate are analyzed at different inclination angles, curvature radii of the front edge of the plate, and sharpness coefficients of the rear part. The pressure field consists of multi-scale spotted structures with a negative values of pressure, corresponding to the positions of vortical elements of the flow, whose spatial and time scales, geometric features, manifestation level, and dissipation rate essentially depend on the angle of inclination of the plate to the horizon, geometrical modification of its edges, and the type of the fluid. Special attention is paid to the fine structure of the flow near the front edge of the plate, which is the area with the most diverse scales of the flow, in which both large-scale and small-scale vertical structures form and actively interact.

Keywords: plate, stratified flow, vortices, fine structure

DOI: 10.1134/S0015462819070152

INTRODUCTION

Starting with the pioneering work by D'Alembert [1] and Euler [2], calculations of flow patterns around obstacles with the evaluation of forces acting on their surface occupy a leading place in theoretical and experimental fluid mechanics due to the fundamental nature of such problems and the wide range of practical applications. One of these is the optimization of structures according to a number of criteria, the expansion of the range of sustainable flight of aircraft, submarines, and surface vehicles, the development of reliable control systems ensuring stability in a wide range of flight and environment conditions, etc.

Particular attention is paid to calculating the flow around obstacles of a fairly simple form, e.g., plate, cylinder, sphere, etc., which are often studied to verify numerical algorithms, improve methods of flow control [3], analyze flow structuring and turbulence mechanisms [4], etc. In view of the mathematical complexity of the problem, a number of approximate models of flow around obstacles were developed at the beginning of the last century, including the Blasius solution for a horizontal half-plane in a boundary layer in the homogeneous fluid approximation [5]. As a rule, such approaches do not take edge effects into account, which makes such idealized models applicable only to rough estimates of the flow structure on a part of a surface of a fairly simple form. The Blasius solution, obtained under the assumption of constant pressure along the normal to the surface without taking edge effects into account, was used for more than 100 years to compare with the data of laboratory experiments and numerical simulation. However, the structure and dynamics of the flow around a plate essentially depend on its thickness, the angle of inclination to the horizon, and the quality of the surface, which determines the fields of velocity, pressure, and their gradients.

A number of experimental and numerical studies of flows around horizontal and inclined plates have been conducted to understand the fundamental regularities governing the formation and development of the structure and dynamics of flows. One of the earliest works concerning the vortex formation behind a

plate with sharp edges was performed in [6], where the flow field around a flat plate was analyzed for 18 different angles of attack. Numerical modeling of flows behind an inclined flat plate with sharp edges was performed in [7–10] using various techniques, including DNS, DES, RANS, and LES, which studied the effect of edge-generated vortices on the structure of the wake flow and specificities of the formation and development of successive stages of the transition from stationary to chaotic flow around an inclined plate. Experimental studies on the visualization of the flow structure in the wake behind an inclined flat plate at $\alpha = 15^\circ$ using the phase-averaged laser Doppler anemometry were performed in [11], which showed the dominance in a wake flow of vortex structures detached from the rear edge of the plate and rotating counterclockwise, and whose formation, development, and subsequent transfer are studied in accordance with the successive stages of the vortex formation cycle.

In practice, the structure and dynamics of flows substantially depend on the geometrical irregularities of the obstacle's surface, in particular, thickness, the quality of the front and rear edges, and the inclination angle of the plate, which determines the velocity and pressure fields, as well as their gradients. Although the number of publications concerning the study of flows in the wake behind a plate oriented in the direction of the incident flow is very large, some earlier and recent problems remain unsolved. One of the most relevant problems is the choice of the shape and thickness of the front edge of a straight wing, which was thin in O. Lilienthal's aviation experiments [12] and was thick in the later design of the Wright brothers' aircraft [13], which took a shape similar to the wing profiles in modern aviation. Many studies have been published in recent years on the influence of the geometrical shape of the front and rear edges of plates and wings on the structure and dynamics of the flow [14–16]. Much attention was paid to the study of vortices generated by the front edge during wing flaps, which presumably play a significant role in the mechanism of insect flight [17].

Under natural conditions, the structure and dynamics of flows also depend on the real properties of the fluid, since the density of the fluid in the environment and industrial devices is not constant due to the nonuniformity of distribution of the concentration of solutes or suspended particles, as well as temperature or pressure [18], which, under the action of buoyancy force, leads to the formation of a stable stratification with a buoyancy period ranging from a few seconds in the laboratory conditions to ten minutes in the Earth's atmosphere and hydrosphere [19].

In this paper, using a numerical simulation, we analyze the multi-scale structure of the flow around an inclined plate in a transient flow regime on the basis of the fundamental system of equations of fluid mechanics, which makes it possible to study the flow in a unified formulation. This study is a logical continuation of previous works, in which the structure and dynamics of stratified flows near immobile [20] and uniformly moving horizontal plates in the linear [21] and complete nonlinear formulations [22, 23] were studied.

1. THE SYSTEM OF GOVERNING EQUATIONS

Mathematical modeling of the flow around an inclined plate is based on the fundamental system of equations for a multi-component inhomogeneous incompressible fluid in the Boussinesq approximation. The effects of buoyancy and diffusion of the stratifying component are taken into account, and the effects of heat conduction and energy release due to dissipation are neglected [24]. Thus, the governing equations take the form:

$$\rho = \rho_0\left(\exp\left(-\frac{z}{\Lambda}\right) + s\right),$$
$$\frac{\partial \mathbf{v}}{\partial t} + (\mathbf{v}\cdot\nabla)\mathbf{v} = -\frac{1}{\rho_0}\nabla P + \nu\Delta\mathbf{v} - s\mathbf{g}, \quad \nabla\cdot\mathbf{v} = 0, \tag{1.1}$$
$$\frac{\partial s}{\partial t} + \mathbf{v}\cdot\nabla s = \kappa_s\Delta s + \frac{v_z}{\Lambda}.$$

Here, s is the salinity perturbation, including the salt compression coefficient, $\mathbf{v} = (v_x, v_y, v_z)$ is the induced flow velocity vector, P is the pressure minus hydrostatic one, $\nu = 0.01\,\text{cm}^2/\text{s}$ and $\kappa_s = 1.41\times10^{-5}\,\text{cm}^2/\text{s}$ are the kinematic viscosity and salt diffusion coefficients, and ∇ and Δ are the Hamilton and Laplace operators.

The proven solvability of the two-dimensional equations of fluid mechanics makes it possible to simultaneously carry out calculations for *stratified* (strongly, when $\Lambda = 9.8$ m, $N = 1\ \text{s}^{-1}$, and $T_b = 6.28$ s and

weakly when $\Lambda = 24$ km, $N = 0.02\,\mathrm{s}^{-1}$, and $T_b = 5.2$ min), and for *potentially homogeneous fluids*, in which the density variations are so small ($\Lambda = 10^8$ km, $N = 10^{-5}\ \mathrm{s}^{-1}$, and $T_b = 7.3$ days) that they cannot be registered by existing technical means, but the original mathematical formulation is preserved, as well as for *actually homogeneous media* ($\Lambda = \infty$, $N = 0$, and $T_b = \infty$). In the last case, the fundamental system of equations degenerates in the part of singular components [25].

The physically justified initial and boundary conditions are the no-slip and impermeability conditions on the obstacle's surface for the velocity components and total salinity, as well as the conditions of unperturbed external flow at a sufficiently large distance from the body:

$$\mathbf{v}|_{t\le 0} = \mathbf{v}_1(x,z), \quad s|_{t\le 0} = s_1(x,z), \quad P|_{t\le 0} = P_1(x,z), \quad v_x|_\Sigma = v_z|_\Sigma = 0,$$
$$\left[\frac{\partial s}{\partial \mathbf{n}}\right]_\Sigma = \frac{1}{\Lambda}\frac{\partial z}{\partial \mathbf{n}}, \quad v_x|_{x,z\to\infty} = U, \quad v_z|_{x,z\to\infty} = 0, \tag{1.2}$$

where U is the uniform velocity of the incident flow at infinity; $\mathbf{n}$ is the outward normal vector to the obstacle's surface Σ, which is here a flat plate of length L and thickness h, placed at an angle α to the horizon, as well as a plate with some geometrical modifications of the edges, which are characterized by dimensionless parameters such as the rounding diameter of the plate's front edge, $\tilde{r}_l = 2r_l/h$, and the sharpness coefficient of the rear edge, $\xi = h/h_t$, where h_t is the thickness of the plate at the rear edge; P_1, $\mathbf{v}_1$, and s_1 are the initial perturbations of the fields of the corresponding physical variables, which are determined from the numerical solution of system (1.1) with trivial boundary conditions at infinity and zero gradient of the total salinity along the normal to the plate surface. The so-called diffusion-induced flows, which arise as a result of the interruption of the molecular flow of the stratifying component by the impermeable surface of an immobile obstacle, have been carefully studied by the authors for various geometrical shapes of the obstacle [19, 20].

The system of equations and boundary conditions (1.1) and (1.2) are characterized by a set of parameters that have the dimensions of length (Λ, L, h) and time ($T_b, T_U^L = L/U$) and also contain dissipative coefficients.

Large dynamic scales: the internal wavelength $\lambda = UT_b$ and the viscous wave size $\Lambda_\nu = \sqrt[3]{g\nu}/N = \sqrt[3]{\Lambda(\delta_N^\nu)^2}$, reflect the structure of the attached wave field. The fine structure of the flow is characterized by universal microscales $\delta_N^\nu = \sqrt{\nu/N}$ and $\delta_N^{\kappa_s} = \sqrt{\kappa_s/N}$, defined by dissipative coefficients and buoyancy frequency (analogs of the Stokes scale on an oscillating surface, $\delta_\omega^\nu = \sqrt{\nu/\omega}$). Another pair: the Prandtl and Peclet scales, are determined by dissipative coefficients and the velocity of the body: $\delta_U^\nu = \nu/U$ and $\delta_U^{\kappa_s} = \kappa_s/U$ [21, 25].

The ratios of the intrinsic scales of the problem are specified as characteristic dimensionless combinations: the Reynolds number $\mathrm{Re}_U = UL/\nu = L/\delta_U^\nu \gg 1$, the internal Froude number $\mathrm{Fr} = U/NL$, the Peclet number $\mathrm{Pe}_U = L/\delta_U^{\kappa_s} \gg \mathrm{Re}_U$, the sharpness coefficient $\xi_p = L/h$, and coefficient specific for stratified flows. The additional dimensionless ratios include the scale ratio $C = \Lambda/L$: the ratio of the buoyancy scale Λ to the obstacle size L; this is an analogue of the inverse Atwood number $\mathrm{At}^{-1} = (\rho_1 + \rho_2)/(\rho_1 - \rho_2)$ for continuously stratified media.

Such a variety of length scales with significant differences in values indicates the complexity of the internal structure of even such a slow flow induced by small buoyancy forces, which arise as a result of the spatial nonuniformity of the molecular flow of the stratifying component. Large scales define the minimum sizes of the observation and computation domains that must contain the structural elements under study: outrunning perturbations, wake, waves, vortices, and the microscales determine the cell size and time step. At low velocities U of the plate, the critical microscale is the Stokes scale and, at high velocities, the Prandtl scale.

2. NUMERICAL SOLUTION

System of equations (1.1) with boundary conditions (1.2) was solved numerically using our solvers and libraries of dynamic meshes as part of an open source OpenFOAM software package based on the finite volume method [26]. For the discretization of the convective terms and the time derivative, we used a limited TVD scheme and an implicit three-point second-order backward difference scheme, respectively,

which provide minimal numerical diffusion, the absence of non-physical oscillations of the solution, and good time resolution of the physical process. In orthogonal regions of the mesh, the diffusion terms are discretized on the basis of the Gauss theorem, and the normal gradient to the surface is calculated from the edge of the computational cell using second-order interpolation of the vector connecting the centers of two adjacent cells. In non-orthogonal areas of the computational mesh, an iterative procedure with a user-specified number of loops correcting the errors caused by the skewing of the mesh.

Two different approaches have been implemented in this numerical simulation. The first consists in imposing the boundary conditions for the free flow and zero gradient at the inflow and outflow boundaries of the computational domain, respectively, while the positions of the cells of the computational mesh and the obstacles remain unchanged. The second approach, in which the plate executes a uniform motion in a steady fluid, is implemented using dynamic computational mesh methods within the OpenFOAM package, which makes it possible to accurately reproduce the conditions of a laboratory experiment similar to those implemented in the Fluid Mechanics Laboratory of the Ishlinsky Institute for Problems in Mechanics of the Russian Academy of Sciences [27]. This approach also makes it possible to avoid the nonphysical perturbations arising at the outer boundaries of the computational domain and to adequately model the structure and dynamics of the flow at the initial stage of the plate's motion. Both approaches give slightly different results at the initial stage, but they are in good agreement at large times, when some repeating patterns can be distinguished on the background of the general unsteady flow.

The algorithm for constructing an orthogonal computational mesh around a plate oriented at an arbitrary angle to the horizon consists in creating separate blocks of the mesh, including an internal cylinder rotating with the plate when its angular position changes, a mesh block attached to the cylinder and complementing it to a parallelepiped, and two more blocks, connected to the parallelepiped on both sides. When the inclined plate moves, the central cylinder and the adjacent mesh blocks move with the plate, while the side mesh blocks are compressed and stretched, respectively, so that the vertical boundaries at the inflow and outflow boundaries remain unchanged.

The spatial sizes of the computational cells were chosen from the condition of adequate resolution of the smallest flow components associated with the stratification and diffusion effects, which impose significant restrictions on the minimum spatial step: the high-gradient areas of the flow should accommodate at least several computational cells in the minimum linear scale of the problem. The computational time step is determined from the Courant condition $\mathrm{Co} = |\mathbf{v}|\Delta t/\Delta r \le 1$, where Δr is the minimum size of the computational cell and $\mathbf{v}$ is the local flow velocity.

3. CALCULATION RESULTS

The calculations were performed for four types of fluids, including strongly ($N = 1.2\ \mathrm{s}^{-1}$) and weakly ($N = 0.1\ \mathrm{s}^{-1}$) stratified, as well as potentially ($N = 10^{-5}\ \mathrm{s}^{-1}$) and actually ($N = 0$) homogeneously fluids. Density variations in a potentially homogeneous fluid are infinitesimal, but the original mathematical formulation is preserved in this case, whereas, in an fully homogeneous fluid, the density is considered constant and the fundamental system of equations degenerates in the singular components [24, 25].

The structure of a stratified flow around an inclined plate is significantly transformed with increasing velocity of the plate, starting from multi-level diffusion-induced circulation flows that occur when molecular flow is disturbed by an impermeable immobile obstacle [19, 20] to complex unsteady vertical and fine-structured regimes at relatively large Reynolds numbers, when all components of the flow are involved in a complex nonlinear interaction [22]. We can distinguish a number of typical flow regimes, depending on the prevalence of one or another structural component of the flow, such as vortices, which are common to all types of fluids, and internal waves, outrunning perturbations, and thin interlayers typical of stratified media [23].

Of the most practical significance are studies of an unsteady vortical regime around obstacles at relatively large Reynolds number. Figure 1 shows instantaneous patterns of the pressure perturbation field at different inclinations of the plate to the horizon for two types of fluid: highly stratified and potentially homogeneous. These patterns demonstrate a number of common features, including an increase in pressure in front of the obstacle and a pressure drop in the spotty structures around the plate, which are localized at the centers of the vortex elements generated by the front edge of the plate. The maximum and minimum pressure values and their location in space essentially depend on the angular position of the plate relative to the horizon and the type of fluid.

All components of the flow actively interact with each other, with the fine structure, and even with attached internal waves, which, in this case, significantly exceed the observation region. Even at small

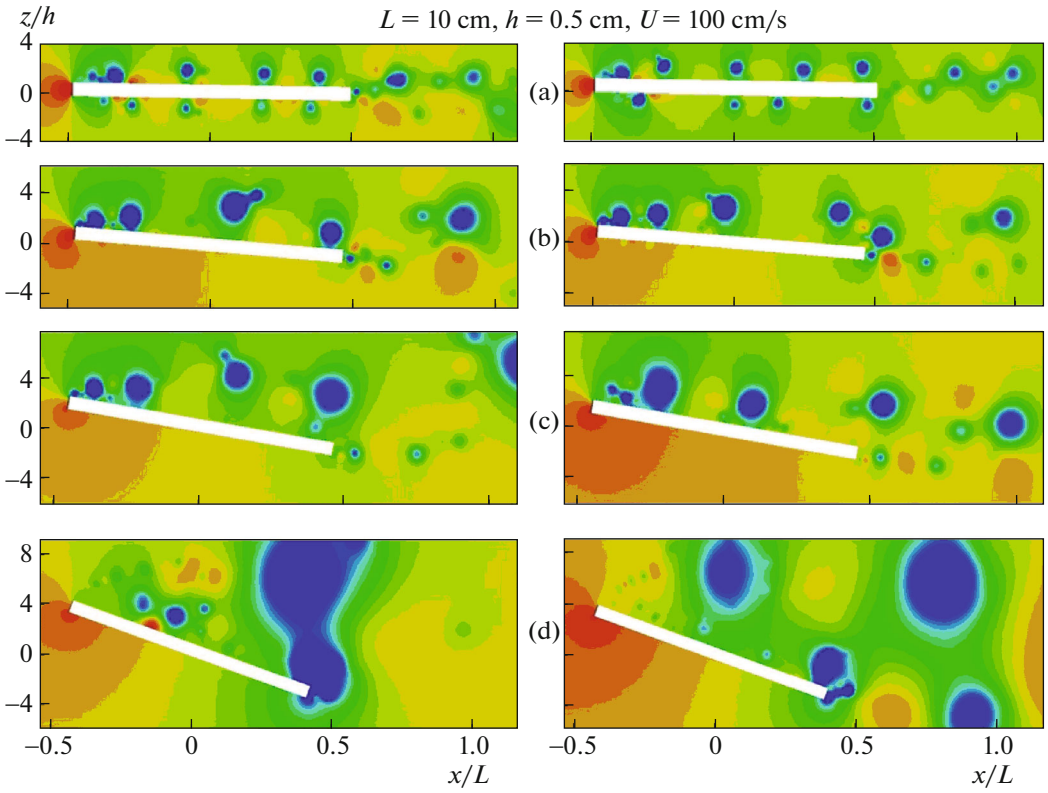

Fig. 1. Instantaneous patterns of pressure perturbation field around an inclined plate for different inclination angles to the horizon: $\alpha = 1°, 5°, 10°, 20°$ (a–d), (left) highly stratified fluid and (right) potentially homogeneous fluid.

inclination angles of the plate, the vortex dynamics noticeably differ in the areas above and below the plate, so that the intensity and scale of the vortices generated by the upper boundary of the front edge and drifting downstream along its surface are noticeably larger in the area above the plate (Fig. 1a). In this case, the vortices under the plate are seen more clearly in the case of a potentially homogeneous fluid, which is explained by the overwhelming influence of the stratification effects.

With increasing inclination angle of the plate, the vortex dynamics of the flow on its lower upstream side is suppressed by the effect of the incident flow, while the scales of the vortex structures forming above the upper side of the plate and in its wake increase (Figs. 1b–1d)). The differences in the intensity, positions, scales, and decay rates of the generated vortex structures for different types of fluids under consideration increase with increasing inclination angle of the plate.

The flow around an inclined plate is a complex multiscale nonstationary physical process, accompanied by the interaction of large- and small-scale components with each other and with the incident flow. All components of the flow are characterized by their own geometry, spatial and temporal scales, manifestation level, and dissipation rate, which must be carefully studied both theoretically and experimentally with allowance for the effects of diffusion, heat conduction, and compressibility, as well as with control of the observability criterion and resolution of all different-scale components of the flow.

Of particular scientific interest is the study of the fine structure of the flow near the front edge of an inclined plate, which is the most diverse-scale region of the flow, where both large and small vortex elements, which actively interact with each other, are formed. The fine structure of the flow near the front edge of an inclined plate is illustrated by instantaneous patterns of the horizontal component of the density gradient $\partial\rho/\partial x$ and the baroclinic vorticity generation rate $\dot{\Omega} = \nabla P \times \nabla(\rho^{-1})$, the fields of which are shown in Fig. 2. Amplification of images in a specific region of the flow makes it possible to identify the complex small-scale structure of the fields and evaluate the geometrical features of the structural elements. Each physical variable entering into the original system of equations reveals some new important features of the flow, favoring a better understanding of the general regularities of the physical process under consideration.

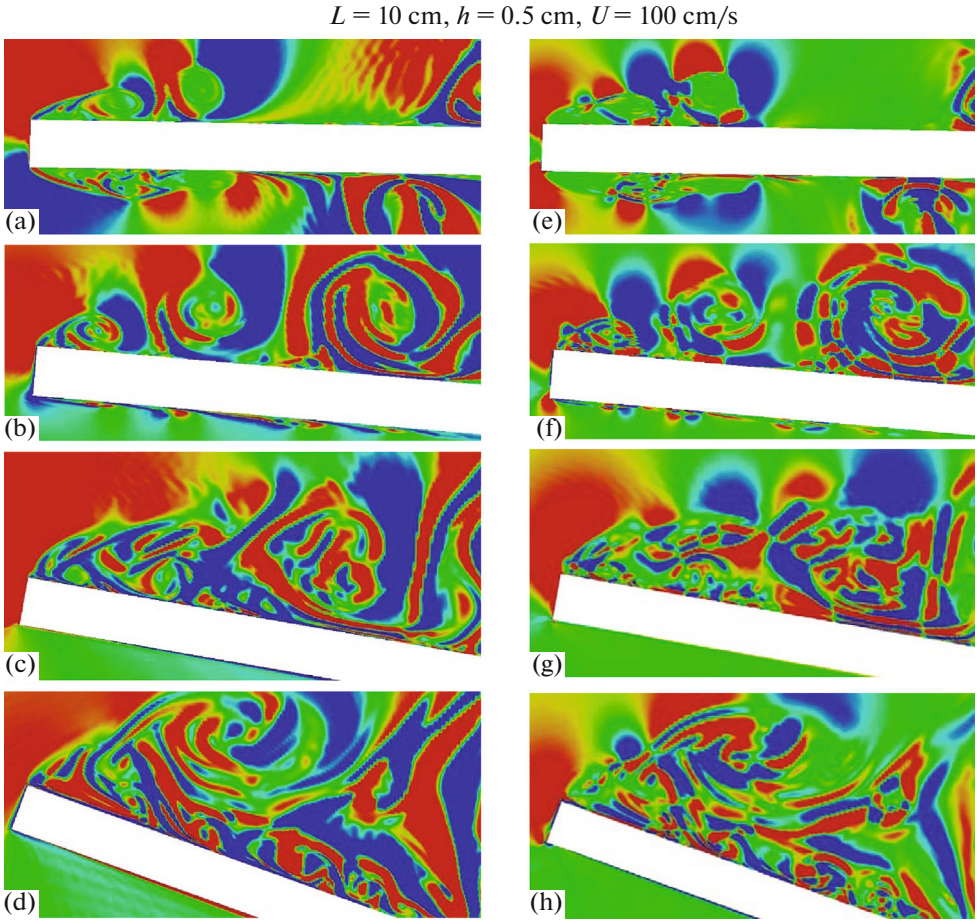

Fig. 2. (a–d) Instantaneous pattern of the horizontal component of the density gradient field and (e–h) baroclinic vorticity generation rate of near the front edge of an inclined plate for different angles of inclination to the horizon in a highly stratified fluid (top down: $\alpha = 1°, 5°, 10°, 20°$).

The field patterns of the horizontal component of the density gradient, which is linearly dependent on the refractive index of light visualized in laboratory experiments using schlieren [27], have a complex fine structure due to the small ratio of diffusion and viscosity coefficients (left side of Fig. 2). The fine-structured layered elements of both signs are localized mainly on the vortex shells and in the regions of the flow with intense vortex interactions. The larger the plate inclination angle to the horizon, the more complex the field structure and the greater the length of the observed layered elements. For $\alpha \geq 10°$, perturbations of the flow on the upstream side of the plates are suppressed by the incident flow, while the field structure over the downstream side becomes much more complicated due to the development of multiple vortex interactions, accompanied by merging, splitting, and complex transformations of different-scale vortex elements of the flow.

The field of baroclinic vorticity generation rate, the patterns of which are shown in Fig. 2 on the right, is determined, according to the Bjerknes theorem, by the noncollinearity of pressure and density gradients. This field is the most complex and structured in flows of inhomogeneous fluids. In the vicinity of the front edge of the plate and in front of the body, there are areas of generation and dissipation of vorticity with scales much smaller than the plate thickness. With increasing inclination angle, the structural elements become thinner and much more complicated: a number of multiple fine-structured regions of amplification and attenuation of vorticity, which gradually elongate with their downstream motion, appear. The geometry of the field of the baroclinic vorticity generation rate explains the dynamics of formation of the fine structure of the vortex flow, as well as the mechanism of field splitting into a series of layered structures clearly observed in the shadowgrams of stratified flows in laboratory experiments [21, 27].

Of great practical interest is the analysis of the structure and dynamics of a stratified flow in a nonstationary vortex regime, in which temporal and spatial scales, manifestation level, and dissipation rate of the forming vortex structures essentially depend on the geometrical shape of the plate edges. The calculation results presented below illustrate instantaneous patterns of the vorticity, pressure, and density gradient fields, which allow a comprehensive analysis of the structure and dynamics of the flow for different curvature radii of the front edge and sharpness of the rear edges of the plate.

The front and rear edges of a horizontal plate are special areas of the flow in which the vorticity vector $\mathbf{\Omega} = \mathrm{curl}\mathbf{v}$ is generated due to the general reorganization of the velocity field and the baroclinic effects. Vortex structures form at the front edge of a rectangular plate with sharp edges with a frequency of about 4 Hz, then detach from its surface at some distance downstream and attach again to the surface at the center of the plate (upper part of Fig. 3a). Then the vortices generated by the front edge drift downstream along the surface and interact with the vortex street that forms in the wake behind the rear edge of the plate with an oscillation frequency of about 5 Hz. As a result of multiple complex interactions of two vortex systems in the wake flow, a new system is formed with a wake frequency of approximately two times lower than that of the original vortex street. It can be seen that the vortices from the front edge and the vortex street in the wake of a rectangular plate with sharp edges are clearly delineated and have an average spatial scale comparable to the thickness of the plate.

With increasing curvature radius of the edge, the vortex structures decrease in scale and intensity and take more diffuse and elongated forms as they move downstream (upper part of Fig. 3b). At the maximum radius of the front edge, the scales of the vortices decrease almost by a factor of two in comparison with a plate with sharp edges and, as they move downstream, take the form of attenuating wave perturbations. In this case, the vortices from the front edge dissipate fairly quickly, even before reaching the rear edge of the plate, and, therefore, do not have a significant effect on the wake, which, in this case, preserves the structure of the primary vortex street.

The patterns of the pressure field for all considered configurations of the plate edges (lower part of Fig. 3) demonstrate a number of common features, including an increase in pressure in front of the obstacle and a pressure drop in spotty structures around the plate, which are localized at the centers of the vortex elements generated by the plate edges. The patterns presented show that the intensity, spatial scales, manifestation level, and dissipation rate of the typical structural elements of the pressure field essentially depend on the considered geometrical configuration of the plate edges.

With increasing curvature radius of the front edge, the high pressure area in front of the obstacle and the spotty low-pressure structures above and under the plate are significantly reduced in intensity and scale due to the smoothing and stabilizing effect of the rounded edge on the vortex dynamics. In the case of a maximally rounded front edge of the plate (lower part of Fig. 3c), the dynamics of the wake flow is most intense due to the minimal influence of the downstream-drifting vortices from the front edge on the wake flow, which preserves the primary structure of the vortex street. In the case of a plate with a rounded front edge and a sharp rear edge (bottom of Fig. 3e), whose shape is closest to the typical airfoil, all perturbations of the pressure field practically disappear at a distance from the rear edge of about half the plate length and the vortex dynamics of the flow becomes least intense and least-scale in comparison with the other considered geometrical configurations of the plate.

Each individual physical variable entering into the original system of equations reveals its own aspect of the physical phenomenon under consideration, which, in general, contributes to a more complete understanding of the physical mechanisms underlying the formation and development of stratified flows near obstacles. The most general and complete analysis of the physical process should be based on the fundamental system of equations, which most comprehensively reveals the features of the physical process thanks to the extended set of physical variables entering into the system [25].

From the field patterns of the horizontal component of the density gradient shown in Fig. 4 for different geometrical configurations of the front and rear edges of the plate, one can obtain additional information on the fine-structured elements of the flow, which are practically indistinguishable in the fields of other physical variables. Shadow imaging methods reveal a wide variety of fine-structured components around moving bodies in a stratified fluid, including ligaments: small-scale links, interfaces, shells, fibers, etc., which are very similar to those observed in the calculated patterns of the horizontal component of the density gradient, which linearly depend on the refractive index of light detected in the laboratory experiments [21, 25].

The field patterns consist of a multitude of small-scale multilayered structures of both signs, which are oriented mainly along the streamlines of the vortex flow elements, forming a system of spiral curls typical of vortices. Fine-structured elements are also localized in the areas of the flow where various flow components actively interact with each other, the incident flow, and the obstacle's surface. The fineness of the

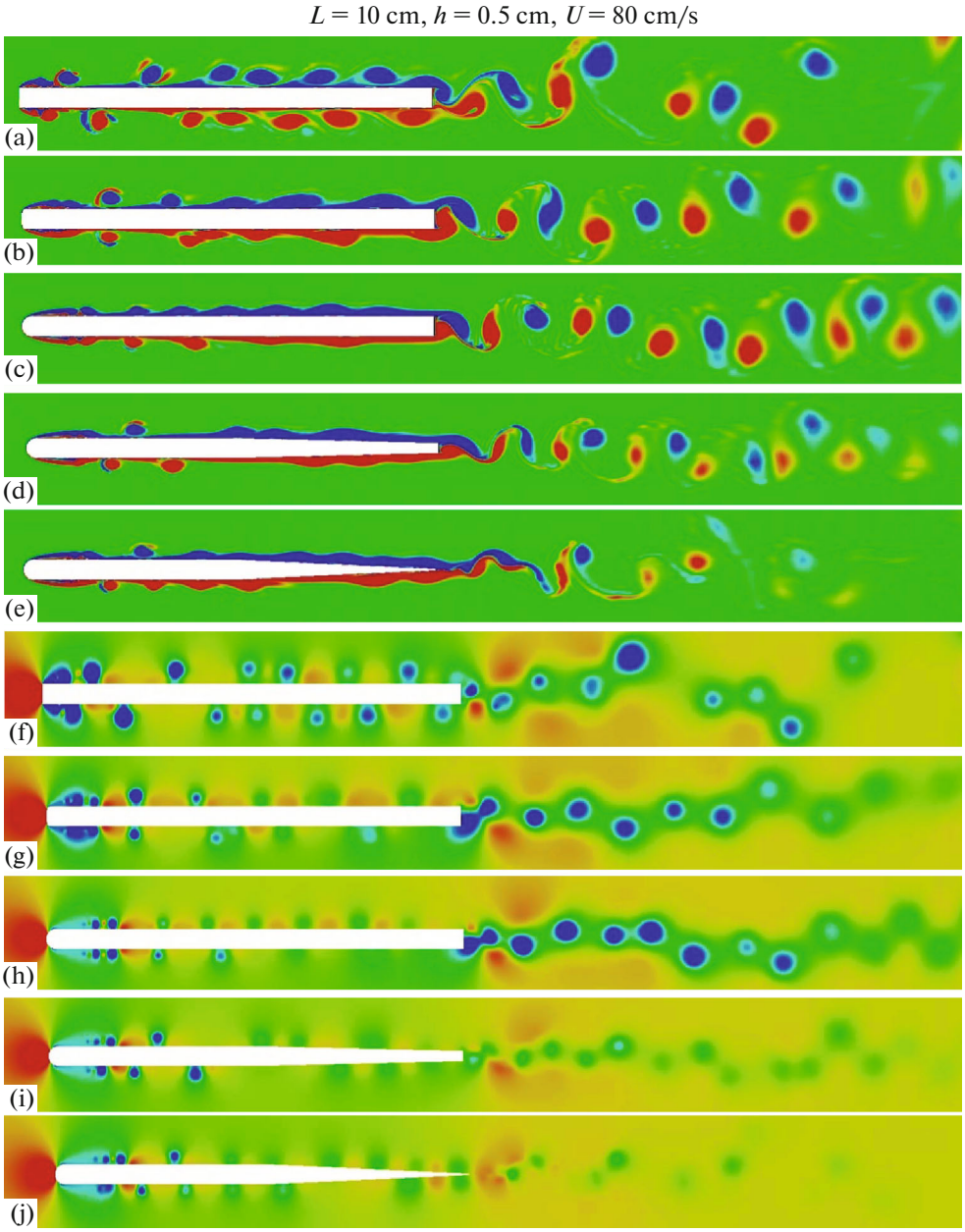

Fig. 3. Instantaneous patterns of the (a–e) vorticity and (f–j) pressure fields near the horizontal plate with different geometrical modifications of its front and rear edges: $(\tilde{\eta},\xi) = (0, 1), (0.4, 1), (1, 1), (1, 2), (1, 10)$.

field structure of the horizontal component of the density gradient is explained by the smallness of the ratio of the diffusion and kinematic viscosity coefficients.

The shortest and finest structures are concentrated near a rectangular horizontal plate with sharp edges in the shells of the vortices generated by its front edge, while, in the wake flow, these structures begin to lengthen, thicken, and become more complicated as they develop downstream from the rear edge of the plate (Fig. 4a). The curvature of the front edge affects the number of fine-structured elements in the area of the flow above and below the plate within the specified range of the horizontal component of the density gradient (Figs. 4b and 4c). At the same time, perturbations of the field are well-defined in the entire region of visualization of the wake flow with all considered geometrical configurations, in contrast to the patterns of the vorticity and pressure fields, in which, in the case of an airfoil-type plate, wake perturbations are hardly distinguishable (upper part of Fig. 3 and lower part of Fig. 3e).

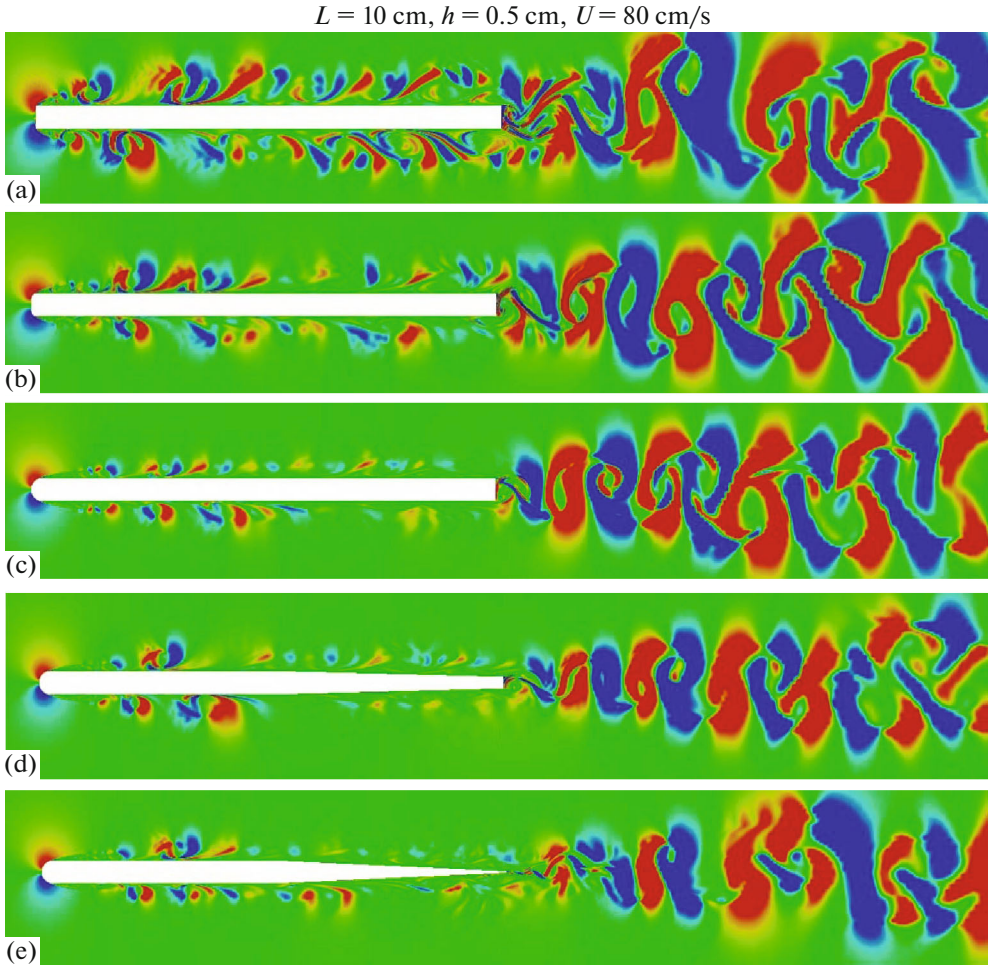

Fig. 4. Instantaneous field patterns of the horizontal component of the density gradient near the horizontal plate in a continuously stratified fluid with various modifications of its leading and trailing edges: $(\tilde{\eta},\xi) = (0, 1), (0.4, 1), (1, 1), (1, 2), (1, 10)$ (a–e).

Pressure distributions on the upper side of the plate are shown in Fig. 5 for three different geometrical configurations of plate edges. The distribution curves are essentially nonmonotonic, which reflects the typical structure of a vortex flow. In the case of a rectangular plate with sharp edges, the variations in pressure near the front edge are about three times greater than in other considered configurations of the plate edges. The pressure fluctuation amplitudes weaken with approaching the rear edge of the airfoil-type plate

Table 1. Integral values of drag, lift, and twisting moment for various modifications of the front and rear edges of the plate

$\tilde{\eta}$	ξ	C_D	C_L	$-C_M$
0	1	0.0322	0.0935	0.0136
0.04	1	0.0311	0.0912	0.0128
0.4	1	0.0254	0.0844	0.0106
0.8	1	0.0252	0.0783	0.0092
1	1	0.0251	0.0752	0.0083
1	2	0.0125	0.0743	0.0126
1	4	0.0110	0.0721	0.0145
1	10	0.0104	0.0693	0.0162

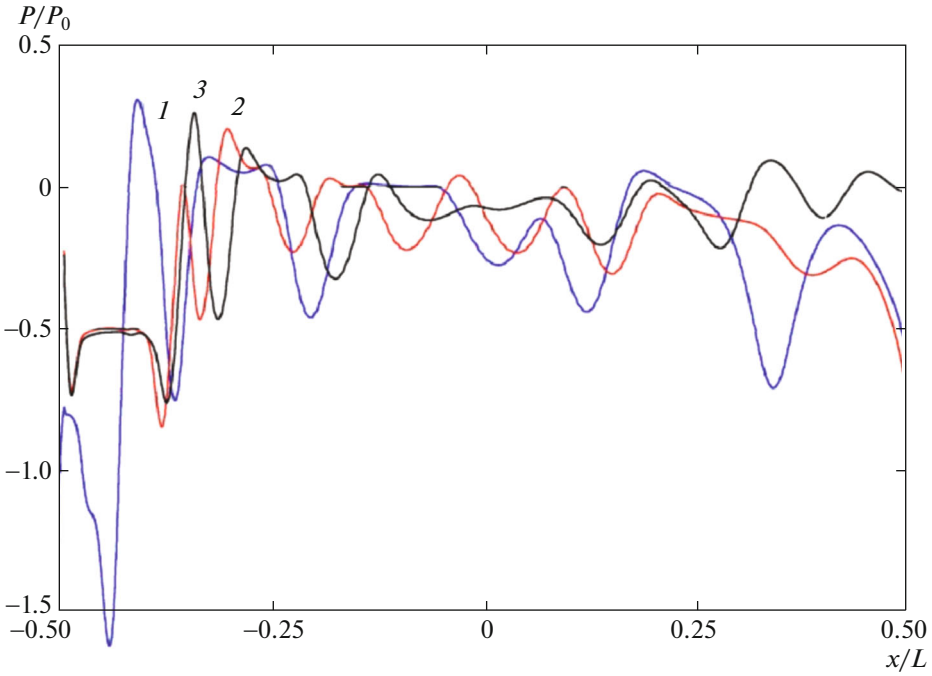

Fig. 5. Pressure distribution on the upper side of a horizontal plate with different modifications of its front and rear edges: $L = 10$ cm, $h = 0.5$ cm, $U = 80$ cm/s, $(\tilde{r}_1,\xi) = (1)$ (0.01, 1), (2) (1, 1), and (3) (1, 10).

(curve *3*), while, in the case of a rectangular plate, the amplitudes of oscillations, on the contrary, increase downstream (curves *1* and *2*).

The integral values of the drag C_D, lift C_L, and twisting moment C_M are presented in Table 1 for different configurations of the front and rear edges of the plate. The values of C_L and C_M were calculated by integrating the corresponding local values only over the upper part of the plate surface, since the integration over the entire surface of a symmetric obstacle gives values comparable to the computational error. It can be seen that an increase in the radius of curvature and the sharpness coefficient of the plate leads to a monotonic decrease in the drag and lift. The integral twisting moment takes negative values, i.e., the incident flow strives to turn the upper side of the plate clockwise.

CONCLUSIONS

The approach developed in this work is based on the numerical solution of a system of differential equations of an incompressible viscous stratified fluid using our solvers and libraries of the OpenFOAM software package, which makes it possible to study the flow of both continuously stratified and homogeneous viscous incompressible fluids in a unified formulation. Each additional physical variable resolved by the original system of equations reveals some new important features of the flow, which contributes to a better understanding of the physical processes under study.

The instantaneous field patterns of perturbation of pressure behind an inclined plate were studied in an unsteady vortex regime for both stratified and homogeneous fluids at different inclination angles of the plate to the horizon. The pictures consist of multiscale spotty structures with negative pressure, which correspond to the location of the elements of the vortex flow with spatial and temporal scales, which also essentially depend on the inclination angle of the plate to the horizon and the type of fluid.

Instantaneous patterns of the vorticity, pressure gradient, and density fields, as well as of forces and twisting moment acting on the plate surface, were analyzed for different radii of curvature of the front edge and the sharpness of the rear edge of the plate. The vortices generated by the rounded front edge are much smaller in scale and rapidly decay downstream, so that the character of the wake preserves its original vortex structure. The perturbations of the flow behind an airfoil-type plate practically disappear downstream at a distance of less than half the length of the plate from the rear edge.

The patterns of the horizontal component of the density gradient field, which describe the fine structure of the flow, consist of many small-scale multilayer structures of both signs, oriented mainly along the streamlines of the elements of the vortex flow, as well as localized in the areas of the flow with active interaction of various components of the flow with the incident flow and plate surface. The perturbations of this field are well-defined in the wake region for all considered geometrical configurations of the plate, whereas, in the case of an airfoil-type plate, perturbations of the wake in the structure of the vorticity and pressure fields are relatively weak.

Instantaneous patterns of the fields under study are characterized by their own geometry, spatial and temporal scales, manifestation level, and dissipation rate, describe the structure and dynamics of the flow from various physical aspects, and explain the mechanisms of formation of the vortex structure and splitting of the flow into a number of fine layered structures clearly observed in the experiments. The flow around a plate of finite length in the general formulation is a complex physical process, which requires detailed experimental and theoretical study with allowance for the diffusion, thermal conductivity, and compressibility effects, as well as with control of criteria of observability and resolution of all different-scale components of the flow.

ACKNOWLEDGMENTS

This work was performed using the services and equipment of the Center for Collective Use of Super High Performance Computer Resources of Moscow State University, as well as the Center for Collective Use "Complex of Modeling and Data Processing of Mega-Class Research Facilities" of the National Research Center "Kurchatov Institute."

FUNDING

The work of Yu.D. Chashechkin was supported in part by the Russian Foundation for Basic Research (grant no. 18-05-00870) and the state budget of the Russian Federation (state task no. AAAA-A17-117021310378-8).

REFERENCES

1. D'Alembert, J., *Réflexions sur la cause générale des vents,* Paris: David, 1747.
2. Euler, L., Principes généraux du mouvement des fluids, *Mémoires de l'Academié royalle des sciences et belles letters,* Berlin, 1757, vol. 11, pp. 274–315.
3. Gaifullin, A.M. and Zubtsov, A.V., Asymptotic structure of unsteady flow over a semi-infinite plate with a moving surface, *Fluid Dyn.,* 2013, vol. 48, no. 1, pp. 77–88.
4. Liu, C., Yan, Y., and Lu, P., Physics of turbulence generation and sustenance in a boundary layer, *Comput. Fluids,* 2014, vol. 102, pp. 353–384.
5. Schlichting, H., *Boundary-Layer Theory,* New York: McGraw-Hill, 1955.
6. Fage, A. and Johansen, F., On the flow of air behind an inclined flat plate of infinite span, *Brit. Aero. Res. Coun. Rep. Memo,* 1927, vol. 1104, pp. 81–106.
7. Jackson, C., Finite-element study of the onset of vortex shedding in flow past variously shaped bodies, *J. Fluid Mech.,* 1987, vol. 182, pp. 23–45.
8. Lam, K., Phase-locked eduction of vortex shedding in flow past an inclined flat plate, *Phys. Fluids,* 1996, vol. 8, pp. 1159–1168.
9. Breuer, M. and Jovicic, N., Separated flow around a flat plate at high incidence: an LES investigation, *J. Turbul.,* 2001, vol. 2, pp. 1–15.
10. Breuer, M., Jovicic, N., and Mazaev, K., Comparison of DES, RANS and LES for the separated flow around a flat plate at high incidence, *Int. J. Num. Meth. Fluids,* 2003, vol. 41, pp. 357–388.
11. Zhang, J., Liu, N., and Lu, X., Route to a chaotic state in fluid flow past an inclined flat plate, *Phys. Rev. E,* 2009, vol. 79 (045306), pp. 1–4.
12. Lilienthal, O., *Die Flugapparate, algemeine Gesichtspunkte bei deren Herstellung und Anwendung,* Berlin: Mayer & Müller, 1894.
13. Wright, W. and Wright, O., Pioneering aviation works of Wright Brothers. http://www.paperlessarchives.com/wright_brothers_papers.html.
14. Hanson, R., Buckley, H., and Lavoie, P., Aerodynamic optimization of the flatplate leading edge for experimental studies of laminar and transitional boundary layers, *Exp. Fluids,* 2012, vol. 53, pp. 863–871.
15. Hasheminejad, S., Mitsudharmadi, H., and Winoto, S., Effect of flat plate leading edge pattern on structure of streamwise vortices generated in its boundary layer, *J. Flow Control, Meas. Vis.,* 2014, vol. 2, pp. 18–23.

16. Thomareis, N. and Papadakis, G., Effect of trailing edge shape on the separated flow characteristics around an airfoil at low Reynolds number: a numerical study, *Phys. Fluids,* 2017, vol. 29, pp. 014101-1–014101-17.
17. Phillips, N., Knowles, K., and Bomphrey, R., Petiolate wings: effects on the leading-edge vortex in flapping flight, *Interface Focus,* 2017, vol. 7, no. 1, p. 20160084.
18. Landau, L.D. and Lifshitz, E.M., *Fluid Mechanics,* vol. 6: *Course of Theoretical Physics,* Oxford: Pergamon Press, 1987.
19. Chashechkin, Yu. and Zagumennyi, Ia., Non-equilibrium processes in nonhomogeneous fluids under the action of external forces, *Phys. Scr.,* 2013, vol. 155, p. 014010.
20. Zagumennyi, Ya.V. and Chashechkin, Yu.D., Fine structure of unsteady diffusioninduced flow over a fixed plate, *Fluid Dyn.,* 2013, vol. 48, no. 3, pp. 374–388.
21. Bardakov, R.N., Mitkin, V.V., and Chashechkin, Yu.D., Fine structure of a stratified flow near a flat-plate surface, *J. Appl. Mech. Tech. Phys.,* 2007, vol. 48, no. 6, pp. 840–851.
22. Zagumennyi, Ya.V. and Chashechkin, Yu.D., Unsteady vortex pattern in a flow over a flat plate at zero angle of attack (two-dimensional problem), *Fluid Dyn.,* 2016, vol. 51, no. 3, pp. 343–359.
23. Chashechkin, Yu. and Zagumennyi, Ia., Formation of waves, vortices and ligaments in 2D stratified flows around obstacles, *Phys. Scr.,* 2019, vol. 94, no. 5, p.054003.
24. Chashechkin, Yu.D., Hierarchy of the models of classical mechanics of inhomogeneous fluids, *Phys. Oceanog.,* 2011, vol. 20, pp. 317–324.
25. Chashechkin, Yu., Differential fluid mechanics—harmonization of analytical, numerical and laboratory models of flows, *Math. Model. Optimiz. Complex Struct.,* 2016, vol. 40, pp. 61–91.
26. Dimitrieva, N.F. and Zagumennyi, Ya.V., Numerical simulation of stratified flows using OpenFOAM package, *Proc. ISP RAS,* 2014, vol. 26, no. 5, pp. 187–200.
27. Chashechkin, Yu. and Mitkin, V., A visual study on flow pattern around the strip moving uniformly in a continuously stratified fluid, *J. Vis.,* 2004, vol. 7, no. 2, pp. 127–134.

Translated by E. Chernokozhin